



ELSEVIER

Available online at www.sciencedirect.com

SCIENCE @ DIRECT®

Nuclear Instruments and Methods in Physics Research A 499 (2003) 508–520

**NUCLEAR
INSTRUMENTS
& METHODS
IN PHYSICS
RESEARCH**
Section A

www.elsevier.com/locate/nima

PHENIX central arm particle ID detectors

M. Aizawa^a, Y. Akiba^b, R. Begay^c, J. Burward-Hoy^c, R.B. Chappell^d, C.Y. Chi^e,
M. Chiu^e, T. Chujo^{f,a}, D.W. Crook^d, A. Danmura^a, K. Ebisu^g, M.S. Emery^h,
K. Enosawa^a, S. Esumi^a, J. Ferrierra^c, A.D. Frawley^{d,*}, V. Griffin^d, H. Hamagakiⁱ,
H. Hara^g, R.S. Hayano^j, H. Hayashi^a, T.K. Hemmick^c, M. Hibino^k, R. Higuchi^a,
T. Hirano^a, R. Hoade^f, R. Hutter^c, M. Inaba^a, K. Jones^f, S. Kametaniⁱ, S. Kato^a,
M. Kennedy^d, J. Kikuchi^k, A. Kiyomichi^a, K. Koseki^a, M. Kurata-Nishimura^a,
K. Kurita^{l,m}, Y. Kuroki^a, T. Matsumotoⁱ, Y. Miake^a, Y. Miyamoto^a,
G.G. Moscone^h, Y. Nagasaka^g, S. Nishimuraⁱ, M. Ono^a, K. Oyamaⁱ, R. Raynis^f,
T. Sakaguchiⁱ, S. Sakai^a, H. Sako^a, S. Salomone^c, S. Sato^a, K. Shigaki^b,
T. Shimada^a, M. Suzuki-Nara^a, M. Tamai^k, Y. Tanaka^g, H. Tsuruoka^a,
S. Urasawa^a, T. Ushiroda^g, J.W. Walker^h, S. Wang^d, A.L. Wintenberg^h,
L.W. Wright^d, K. Yagi^a, Y. Yokota^a, G.R. Young^h

^a *Institute of Physics, University of Tsukuba, Tsukuba, Ibaraki 305-8571, Japan*

^b *High Energy Accelerator Research Organization, Ibaraki 305-0801, Japan*

^c *SUNY Stony Brook, Stony Brook, NY 11974-3800, USA*

^d *Florida State University, Tallahassee, FL 32306, USA*

^e *Columbia University, New York, NY 10027 and Nevis Laboratories, Irvington, NY 10533, USA*

^f *Brookhaven National Laboratory, Upton, NY 11973-5000, USA*

^g *Nagasaki Institute of Applied Science, Nagasaki 851-0193, Japan*

^h *Oak Ridge National Laboratory, Oak Ridge, TN 37831, USA*

ⁱ *Center for Nuclear Study, University of Tokyo, Tokyo 188-0002, Japan*

^j *Department of Physics, University of Tokyo, Tokyo 113-0033, Japan*

^k *Waseda University, Tokyo 169-8555, Japan*

^l *RIKEN (The Institute of Physical and Chemical Research), Wako, Saitama 351-0198, Japan*

^m *RIKEN BNL Research Center, Brookhaven National Laboratory, Upton, NY 11973-5000, USA*

The PHENIX collaboration

Abstract

The Ring-Imaging Cherenkov (RICH) and the Time-of-Flight (ToF) systems provide identification of charged particles for the PHENIX central arm. The RICH is located between the inner and outer tracking units and is one of the primary devices for identifying electrons among the very large number of charged pions. The ToF is used to identify hadrons and is located between the most outer pad chamber (PC3) and the electromagnetic calorimeter. A Time Zero (T0) counter that enhances charged particle measurements in p-p collisions is described.

*Corresponding author. Tel.: +1-850-644-4034; fax: +1-850-644-4478.

E-mail address: frawley@fsuhip.physics.fsu.edu (A.D. Frawley).

Details of the construction and performance of both the RICH, ToF and T0 are given along with typical results from the first PHENIX data taking run.

Published by Elsevier Science B.V.

PACS: 29.40.Ka; 29.40.Mc; 29.30.Dn; 29.30.Ep

Keywords: Cherenkov detectors; Scintillation detectors; Electron spectroscopy; Charged particle spectroscopy

1. Introduction

The PHENIX detector [1] at the Relativistic Heavy Ion Collider (RHIC) is designed to perform a broad study of A–A, p–A and p–p collisions to investigate nuclear matter under extreme conditions. The central arms of PHENIX measure electrons, photons and hadrons with excellent resolution using tracking detectors [2], Ring Imaging Cherenkov (RICH) and Time-of-Flight (ToF) detectors and electromagnetic calorimeters (EMCal) [3].

Electron detection requires excellent separation of electrons from hadrons over a wide range of momenta from 0.2 to 5.0 GeV/ c or greater. In order to obtain the required redundancy and dynamic range, several different detectors must be used in conjunction. These include the RICH, the EMCal and the Time Expansion Chamber (TEC) in one arm of the central arm tracking system [2]. The RICH is one of the primary devices for separation of electrons from the large numbers of the more copiously produced pions. The ToF system is used to measure charged hadrons over a large momentum range. It can separate pions from kaons up to a momentum of 2.4 GeV/ c . For the measurements of the start timing of ToF in p–p collisions, a T0 counter has been implemented.

2. Ring imaging Cherenkov detector

Each of the PHENIX central arms contains a RICH detector that provides e/π discrimination below the π Cherenkov threshold, which is set at about 4 GeV/ c . In combination with the EMCal in each arm and the TEC in one arm, the goal is to limit the false identification of hadrons as e^+ and e^- to less than $1 \text{ per } 10^4$, for momenta below the

Cherenkov threshold. The EMCal is capable of rejecting about 90% of hadrons at momenta $> 1 \text{ GeV}/c$, and the TEC (present in only one arm of PHENIX) provides dE/dx separation of electrons from pions for momenta below about 1 GeV/ c .

Because the RICH is an electron detector, and because there are several detectors behind it, the amount of material in the RICH within the PHENIX acceptance is of great concern. The very large photon flux for central RHIC collisions, due mostly to π^0 decay, causes e^+e^- pairs to be created in whatever material is inside the RICH acceptance. For this reason the RICH windows, mirrors and even the radiator gas itself, have to be as thin as feasible. As built, the PHENIX RICH detectors have a total thickness of 2% of a radiation length when filled with ethane gas.

2.1. Description of the RICH detector

Fig. 1 contains a cutaway drawing of one of the RICH detectors revealing the internal components. Each RICH detector has a volume of 40 m^3 , with an entrance window area of 8.9 m^2 and an exit window area of 21.6 m^2 . Each detector contains 48 composite mirror panels, forming two intersecting spherical surfaces, with a total reflecting area of 20 m^2 . The spherical mirrors focus Cherenkov light onto two arrays of 1280 Hamamatsu H3171S UV photomultiplier tubes (PMTs), each located on either side of the RICH entrance window. The phototubes are fitted with 2" diameter Winston cones and have magnetic shields that allow them to operate at up to 100 G. The phototube UV glass windows absorb photons of wavelengths below 200 nm. The minimum thickness of radiator gas seen by any particle is 87 cm, the maximum is about 150 cm. The radiator gas is maintained at a pressure of 0.5"

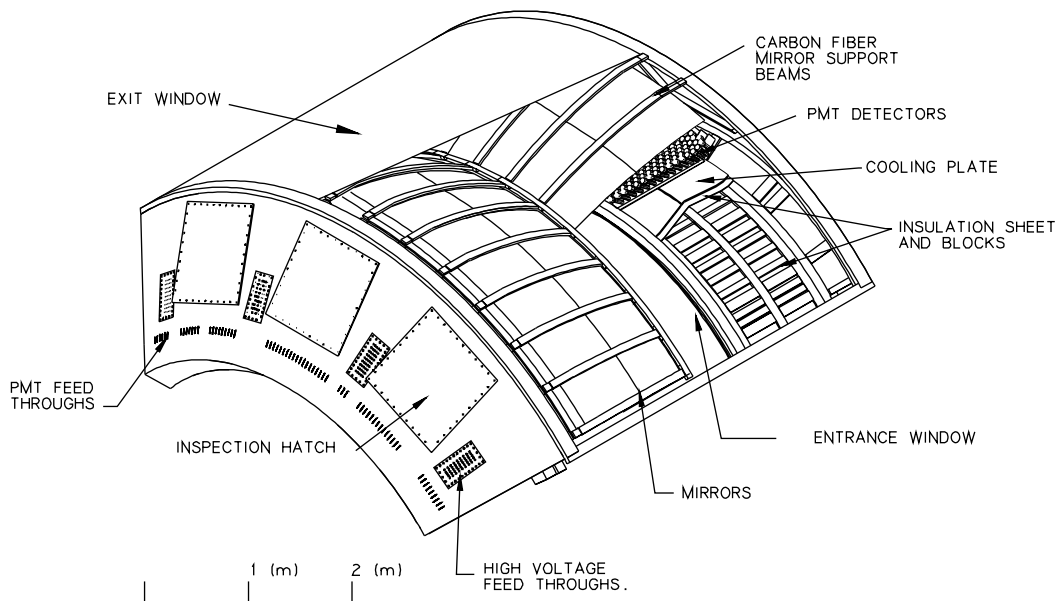


Fig. 1. A cutaway view of one arm of the PHENIX RICH detector.

of water above ambient. The large aluminized Kapton entrance and exit windows are $125\ \mu\text{m}$ thick, and are supported against the internal pressure by graphite-epoxy beams. All gas seals are made using Goretex gaskets. There are black vinyl coated polyester light shields covering the outside of the Kapton windows. The preamplifiers for the signals from the photon detectors are mounted directly on the RICH detector.

The e/π discrimination capabilities of the RICH are determined by three factors: the value of the pion Cherenkov threshold, the statistical fluctuations in the number of photoelectrons produced by an electron in the RICH and the background counting rates in the RICH. Since dark current noise produces only about 0.5 hits per RICH per event, background counting rates are dominated by spurious electrons produced by photon conversions in the PHENIX detector, both inside and outside of the RICH.

Simulations of the RICH response using GEANT show that the gas which provides the best compromise between photon statistics and pion threshold for heavy ion collisions is ethane. In addition, ethane is transparent down to a wavelength of $160\ \text{nm}$, it is not a bright

scintillator, and it has a reasonably low mass. Ethane has a pion Cherenkov threshold of $3.71\ \text{GeV}/c$, and produces an average of 20 photons per ring for a $\beta = 1$ particle, for a path length of $1.2\ \text{m}$. The ring diameter is about $14.5\ \text{cm}$. Since no other gases perform nearly as well, ethane was chosen as the radiator gas for the PHENIX RICH. There are some non-flammable gases that have comparable Cherenkov thresholds and photon yields to ethane. Examples are freon 22 and freon 13. However these gases are very thick (2.1% of a radiation length for freon 22, 2.4% for freon 13). Aside from increasing the thickness of the RICH by a factor of two relative to ethane, simulations show that the electron/pion separation is poorer by a factor of two, due to increased background from photon conversions in the thicker gas.

An alternative radiator gas, most suitable for use in p-p running or in light A-A running, is CO_2 . It has a pion Cherenkov threshold of $4.65\ \text{GeV}/c$ and produces an average of 12 photons per ring for a $\beta = 1$ particle, for a path length of $1.2\ \text{m}$. The ring diameter for CO_2 gas is about $11.8\ \text{cm}$. Simulations show that the e/π separation is poorer by a factor of two for CO_2

relative to ethane, because of the lower photon yield. CO_2 is to be used as the radiator gas during the first several years of operation.

Based on simulations, a reflection angle error of ± 1.5 m rad was chosen as the specification for the RICH mirrors. This sets the large-scale accuracy requirement for the mirror shape, and is not a very stringent requirement. However, to reduce reflectivity losses due to diffractive scattering at the wavelengths of interest for the RICH, namely at about 200 nm, the small-scale RMS surface roughness of the mirror must be kept to 3 nm or less. A bare aluminum surface was used, since oxidation of the surface has a negligible effect on the reflectivity of aluminum for wavelengths above 200 nm.

Because spurious e^+e^- pairs are a significant source of background electrons in the EMCAL, the parts of the mirror array that are within the acceptance of PHENIX had to be as low in mass as possible. A Rohacell foam core and carbon fiber epoxy beams were used for the mirror support structure. The mirror attachment hardware is made mostly of delrin, a plastic. The mirror panels were made using carbon fiber epoxy technology, and the reflective surface was added by replication, a process in which a high quality reflective layer can be transferred from a highly polished master onto a thin layer of epoxy covering a low quality substrate. This technique for making very low mass mirrors was suggested to us by the paper by Egle et al. [4].

The mirror panel substrates were manufactured by ARDCO.¹ They have a radius of curvature of about 401 cm and the panel shapes are defined by lines of latitude and longitude on a spherical surface. The panels are 81.2 cm long with widths that vary from 43.2 to 50.5 cm. The cross-section of a mirror panel is shown in Fig. 2. They consist of 1.25 cm of Rohacell foam with four layers of graphite epoxy on each side. The combined thickness of the four layers of graphite epoxy is 0.7 mm. The mirror surface of each panel also has a gel coat layer on the outside that has been sanded down to 50–100 μm thickness. Each panel

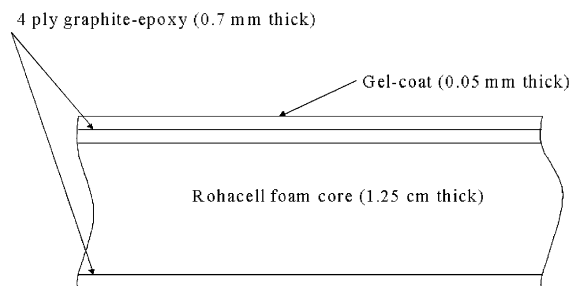


Fig. 2. Cross-section of a mirror panel (not to scale).

weighs either 1200 g (inside mirrors) or 1300 g (outside mirrors) and is 0.53% of a radiation length thick. The panels were molded on a steel master which was polished to a RMS roughness of 2 μm . The master had a radius of curvature of 407 cm, which is larger than the 401 cm radius of the mirror panel. The difference, which was determined by experience, compensates for the small reductions in radius that occur when the panel is separated from the master, and later as a result of the replication process.

Replication of the PHENIX RICH mirrors was performed by OPTICON² using a glass master with a RMS surface roughness of 2.5 nm and a radius of curvature of 408.3 cm. The thickness of the replication epoxy was typically 150 μm . One difficulty encountered in replicating the RICH mirrors was due to the elasticity of the panels. Although the panels are very strong and appear to be quite rigid, it does not require much force to deform them from a spherical shape by 100 μm or more. Some effort was required at OPTICON to learn how to support the panels during replication without deforming them enough to interfere with the replication. Reflectivity tests on a small replicated sample cut from one of the mirror panel substrates showed the reflectivity to be 83% at 200 nm, rising to 90% at 250 nm. Similar reflectivities were observed in later measurements on full sized panels.

All mirrors were tested at OPTICON to determine whether they met the specifications.

¹Advance Ratio Design Company, Inc., 25 Green Street, Chester, PA 19013, USA.

²OPTICON Corporation, 76 Treble Cove Rd, N. Billerica, MA 01862, USA.

Many of the mirrors were also tested at Florida State University after delivery to determine their optical properties. A sample of 45 mirrors was found to have an average radius of curvature of 401.1 cm, with a standard deviation of 2.2 cm. Careful measurements of the image of a point source from eight mirrors gave an average blur-circle of ± 1.5 mrad. This will lead to a position spread due to reflection inaccuracy of ± 2.5 mm at the photon detector array. This is quite small when compared with the Winston cone diameter of 50 mm.

The mirror mounting arrangement allows the mirrors to be aimed after installation in the RICH detector by adjusting the length of three mounting rods. The use of a ball joint for the central mounting point on each mirror, and balls in slots for the other two mounting points, was necessary to avoid the deformation of the mirror panels that would have occurred during adjustment if the ends of the mounting rods were attached rigidly to the back of the mirror. The mirror alignment was done with the RICH detector standing upright in the same orientation as on the PHENIX carriage. The alignment was carried out using a computerized theodolite system (MANCAT). Targets were placed in five locations on the surface of each of the 48 mirror panels and the panels were adjusted to place all of the targets within 0.25 mm of the correct spherical surface.

The H3171S photomultiplier tube has a bi-alkaline photocathode and a line focus 10-stage dynode. The quantum efficiency is 27% at peak, the typical dark current is 10 nA, and the gain is selected to be $> 10^7$. In test beam measurements the timing resolution for a ring was found to be about 250 ps. The photomultiplier tube arrays are divided into modules of 32 phototubes, mounted on water cooled aluminum plates. A module holds its phototubes in two staggered rows of 16 tubes each. When the modules are installed in the RICH, the adjacent staggered rows of tubes with their Winston cones interlock to form a closely packed array. The angles of the phototubes in the modules were chosen on the basis of simulations to maximize the acceptance of photons reflected from the mirrors. The modules are designed so that the two rows

of phototubes can be tilted to one side relative to the module base for installation, then rotated upright to interlock with the phototubes in the previously installed module. One module weighs a total of 70 lbs.

A pulsed LED system was installed in each RICH that allows the photon detectors to be tested. The LED system usually provides a single photon per pulse per detector.

2.2. RICH front-end electronics

The purpose of the RICH Front-End Electronics (FEE) is to measure the Cherenkov rings generated in the gas radiator and imaged on the photon detectors. One interaction produces only a few photoelectrons (typically less than 10), so it is important to locate the electronics near the PMTs to minimize pickup and cable losses. The RICH gas vessel is inaccessible and potentially uses flammable gas, so it is desirable to locate most of the electronics far from the RICH vessel. The solution was to have the RICH preamps mounted on small boards attached to the RICH vessel, with the remainder of the electronics located outside the vessel in a VME 9U crate.

The preamp output drives both a charge and a timing measurement channel. The timing measurement uses a discriminator followed by a TAC while the charge measurement employs a CMOS charge-integrating amplifier followed by a variable-gain amplifier [5]. Both of the above outputs are stored in Analog Memory Units (AMU) [6] clocked at the RHIC beam clock frequency. The analog data is stored in the AMUs and only digitized after the receipt of an accept from the LVL1 trigger. In addition to the AMU/ADC boards the VME 9U crate contains a Controller Board that receives slow control information from ARCNet, and timing and control information from the PHENIX master control system. It also generates headers and trailers for the data packets, provides heap management and distributes timing information. The Readout Board is used to collect the data packets and send them to the Data Collection Modules (DCM). A general description of FEEs and FEMs used in PHENIX is found elsewhere in this volume [7].

2.3. RICH performance

The PHENIX RICH detector was successfully operated in the year-1 RHIC run which took place in the year 2000. The results have been used to evaluate the performance of the RICH. The occupancy of the RICH was low, only about 3.4% even in the most central Au–Au collisions, due to the very high granularity of the detector. Fig. 3 shows the number of photo-electrons per ring (only hits within a radius of 11 cm were used) for electrons identified by ToF in the momentum range of 0.3–0.4 GeV/ c , with the condition that the number of hit phototubes be more than two. The dashed line shows the number of photo-electrons per ring, and the solid line shows the distribution after subtracting the estimated background, shown as the dotted line. The background is estimated by flipping the z -axis of the hit position with respect to the vertex point of $z = 0$. The mean number of photo-electrons per ring is ~ 10.8 , which agrees very well with simulation results and the design goal.

Fig. 4 illustrates electron identification using the RICH detector. In this figure, the ratio of the

energy (measured by the calorimeter) and the momentum of the charged tracks in the transverse momentum range of $1.1 < p_T < 1.2$ GeV/ c are plotted. For all charged tracks, the E/p ratio has a MIP peak at $E/p \sim 0.3$ superimposed on a broad distribution caused by hadronic interactions. When RICH hits are required, a clear peak appears at $E/p = 1.0$, which is the electron signal. The background due to random associations of RICH hits and tracks is estimated and also shown in Fig. 4.

Fig. 5 shows a contour plot of RICH hits associated with tracks reconstructed by the DC. Peripheral events were used for the plot to minimize accidental associations. The ring is seen clearly.

3. ToF counters

PHENIX has a capability for simultaneous measurement of many different probes such as hadrons, leptons and photons. Since hadron production in heavy ion collisions carries the basic information of the properties of the matter, it is

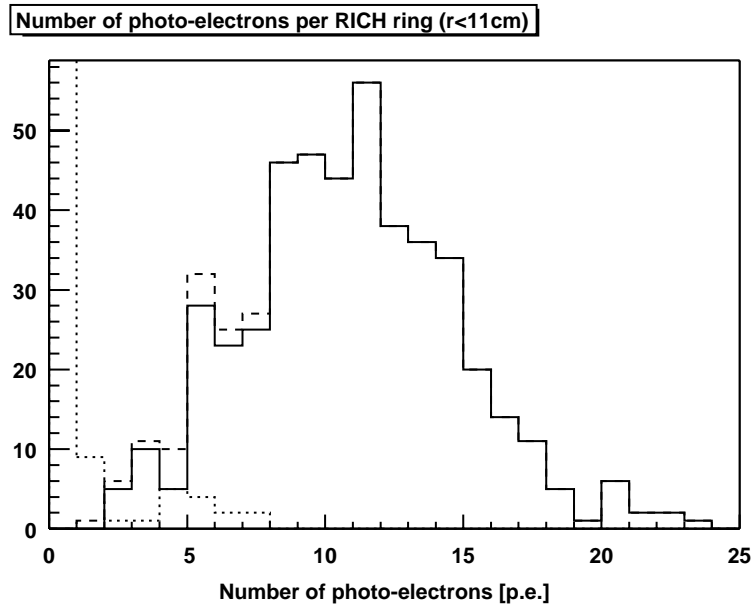


Fig. 3. The dashed line shows the total number of photo-electrons per ring. The solid line shows the distribution after subtracting the estimated background as shown by the dotted line. The mean value of ~ 10.8 is almost identical to that expected from simulation results.

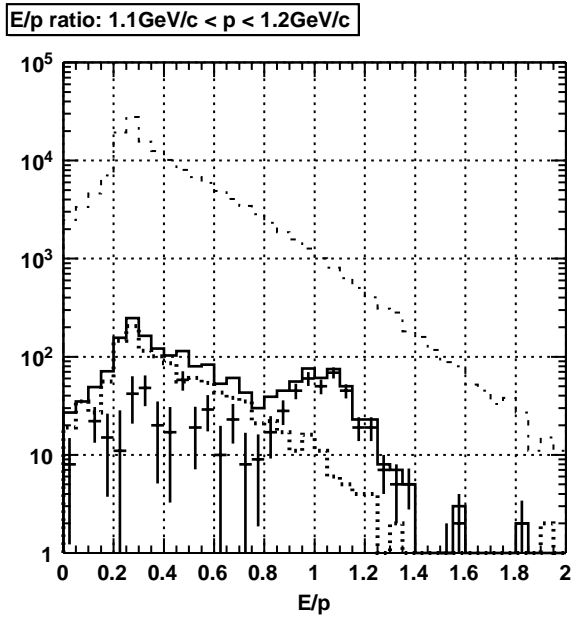


Fig. 4. Ratio of energy and momentum for all Drift Chamber (DC) tracks (dashed-dotted line), tracks associated with RICH hits (solid line), estimated background for tracks with a RICH hit (dotted line), and tracks associated with RICH hits after background subtraction (solid markers). The transverse momentum range is from 1.1 to 1.2 GeV/c.

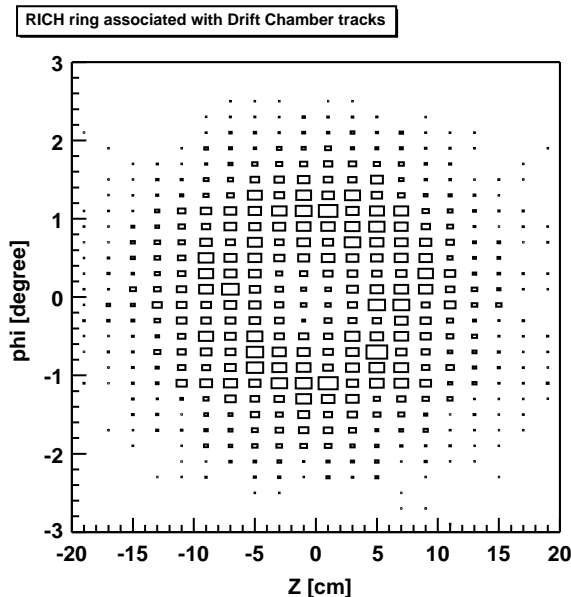


Fig. 5. Contour plot of RICH hits relative to the projected ring centroid from tracking, summed over many tracks.

important to measure identified hadrons in a wide range of p_T . In addition to single particle spectrum measurements, Hanbury–Brown–Twiss (HBT) correlation measurements and measurement of ϕ mesons through the K^+K^- channel are also important to probe the hot and dense matter created in Au–Au collisions at RHIC. For particle identification, ToF measurements, where one compares the particle ToF to the measured momentum of the particle, are one of the most powerful methods for separating particle species. The ToF contains 960 scintillator slats oriented along the r - ϕ direction. Its timing resolution was about 100 ps in the year 2000, the first year of operation of the experiment, which provided a 4σ π/K separation up to 2.4 GeV/c. In this section, we describe the basic design of the ToF counter, the specification of each component and the FEE module. Finally, we present the performance of the ToF detector using data taken in the first year of RHIC operation.

3.1. Detector design

The PHENIX ToF system serves as a primary particle identification device for charged hadrons in PHENIX. It is designed to have about 100 ps timing resolution in order to achieve clear particle separation in the high momentum region, i.e. π/K separation up to 2.4 GeV/c and K/proton separation up to 4.0 GeV/c.

The ToF detector is placed at a distance of 5.1 m from the collision vertex, in between the Pad Chamber (PC3) [2] and the EMCal [3] in the east arm of PHENIX. It is designed to cover the η range ($70^\circ \leq \theta \leq 110^\circ$) of the central detector over 30° in azimuth. The ToF detector consists of 10 panels of ToF walls. One ToF wall consists of 96 segments, each equipped with a plastic scintillator slat and PMTs which are read out at both ends.

The number of segments in the ToF system is determined by minimizing the probability of two or more particles hitting a single segment. For the ToF system design the double hit probability is kept as low as possible. Assuming the charged particle rapidity density to be $dN_{ch}/dy = 1500$, the charged particle multiplicity on the ToF wall is expected to be 9. In order to keep the occupancy

below 10%, the segmentation is about 1000 and the required area of each segment at a distance of 5.1 m away from the vertex is 100 cm^2 .

A total 10 ToF panels, 960 slats of scintillators and 1920 channels of PMTs were installed and operated in the first year of operation. The slat is oriented along the r - ϕ direction and provides time and longitudinal position information of particles that hit the slat. Fig. 6 shows a photo of the ToF detector system mounted on the PHENIX East Arm in the PHENIX experimental hall. All 10 panels of the detector are shown. Fig. 7 shows a schematic view of one panel of the ToF detector. It consists of 96 plastic scintillation counters with PMTs at both ends, light guides and mechanical supports. Scintillator rod and light guides were wrapped with thin aluminum foil and were glued on the honeycomb board. The honeycomb boards are made of paper of a honeycomb structure sandwiched between carbon fiber sheets, which provide a “massless” rigid structure. Scintillators with two different lengths (637.7 and 433.9 mm)

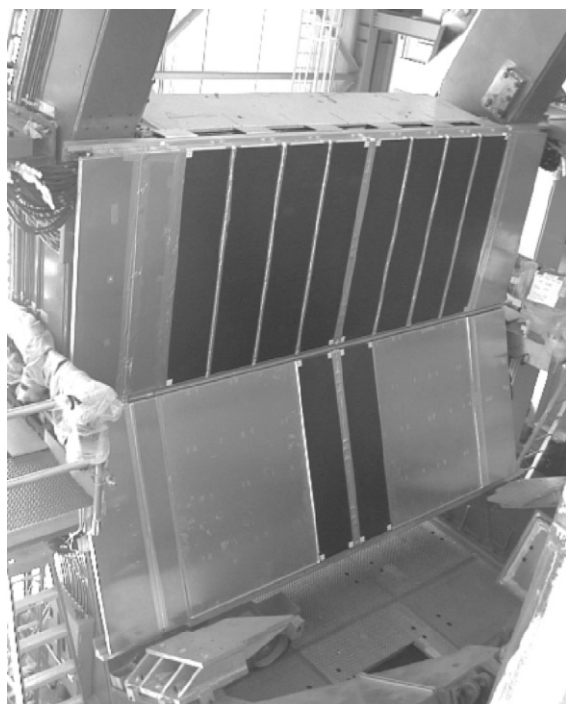


Fig. 6. The ToF detector system mounted on the PHENIX East Arm showing 10 panels of the detector.

are assembled in an alternating fashion in order to avoid geometrical conflicts between the PMTs of neighboring slats. Each end of the scintillator slat is attached with optical glue to a 180° bent light guide. On both sides of one panel, the light guides are bent 90° so as not to conflict with the neighboring PMTs. The scintillator slats are glued on the honeycomb board which consists of carbon fiber sheet and honeycomb paper in order to reduce the amount of material but also provide the wall with sufficient mechanical strength. The signal cables are RG58C/U and the high voltage cables are GXO3173-01. The total radiation length including PMTs and cables is about 6%. Using different lengths of scintillator slats and adoption of bent light guides as described above has allowed us to achieve very small dead space between the ToF slats.

3.2. The ToF scintillator and PMTs

The plastic scintillator used in the ToF is Bicorn BC404, 1.5 cm in width and 1.5 cm in depth. It has good timing characteristics with a moderate attenuation length. The physical constants of this scintillator are given in Table 1.

The ToF system uses Hamamatsu R3478S PMTs. These tubes have a 0.75-in. (19-mm) diameter window of borosilicate glass, an 8 stage linear-focussed dynode structure and a bialkali photocathode. The length of the tube is about 6.7 cm. The relevant physical constants of this tube are given in Table 2. The PMTs are arranged along the direction parallel to the scintillator bar. The magnetic field expected around the ToF system is less than 10 G and its direction is perpendicular to the PMT. The requirement for the μ -metal shielding is therefore not severe. We use a 0.5-mm thick, 7.0-cm long μ -metal shield with an internal diameter of 23 mm. The hit position in the vertical direction (along the slats) is derived from the time difference observed in the signals, read out at the two ends of the slat.

3.3. Front end electronics

The FEE of the ToF are designed to sample the PMT signals at the bunch crossing frequency

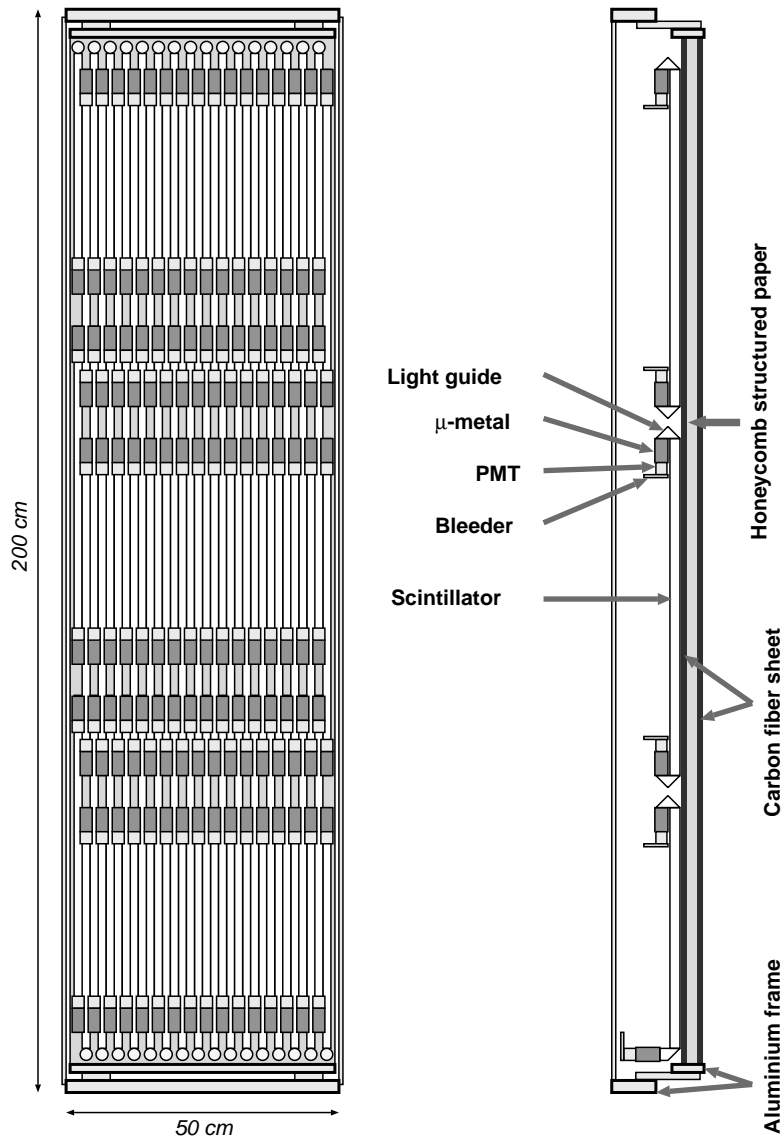


Fig. 7. Schematic diagram of the components of a single ToF panel, which consists of 96 plastic scintillation counters with photomultiplier tubes at both ends, light guides and supports.

(9.4 MHz) of RHIC and store them during the first level trigger latency of $4.24 \mu\text{s}$ corresponding to 40 RHIC bunch crossings. The signal timing from the PMT is determined by a leading edge discriminator followed by a Time-to-Voltage Converter (TVC). The charge information is converted to a voltage by a Charge-to-Voltage Converter (QVC). The analog voltages from the TVC and the QVC

are stored by a switched capacitor Analog Memory Unit (AMU) which stores the information during the latency and buffers up to five accepted events. The stored voltages are digitized by a 12 bit 1.25 MHz ADC. To eliminate the crosstalk between adjacent channels there are two independent readout channels. One is a signal channel and the other is a reference channel which

Table 1
Characteristics of the BC404 scintillator

Physical constant	Value
Light output (% anthracene)	68
Wavelength of maximum emission	408 nm
Decay constant	1.8 ns
Bulk attenuation length	160 cm
Refractive index (n)	1.58

Table 2
Characteristics of the R3478S PMT

Physical constant	Value
Wavelength of maximum response	420 nm
Current amplification	$\sim 10^6$
Anode pulse rise time	1.3 ns
Electron transit time	14 ns
Transit time spread	0.36 ns
High voltage supply	−1800 Vdc

serves as an antenna for crosstalk elimination. By taking the difference between the two channels, there is now no crosstalk in the output. Ref. [7] discusses in detail the specifications and performance of the FEE.

3.4. ToF detector performance from the first run

Particle identification for charged hadrons is performed by combining the information from the DC, PC1, BBC and the ToF. The designed ToF resolution is about 100 ps. This allows us to achieve a PID capability for high momentum particles, a 4σ π/K separation at momenta up to 2.4 GeV/c and a K/p separation up to 4.0 GeV/c. Fig. 8 illustrates the particle separation capabilities of the ToF system. A track is reconstructed from hits in the DC and PC1 that point to the ToF detector. In this reconstruction we use a window for ToF association adjusted so that the residuals between the projection point and the reconstructed ToF hit position is within 2.5 standard deviations.

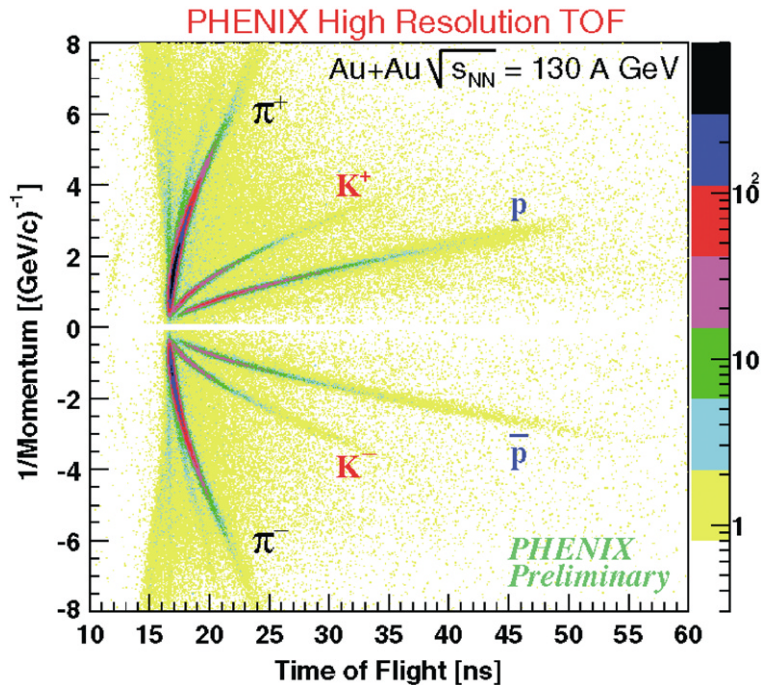


Fig. 8. Contour plot of the ToF versus reciprocal momentum in minimum bias Au–Au collisions at the energy of $\sqrt{s_{NN}} = 130$ GeV. The figure clearly demonstrates the particle identification capability using the ToF detector in the year 2000 data taking period. The flight path is corrected for each track.

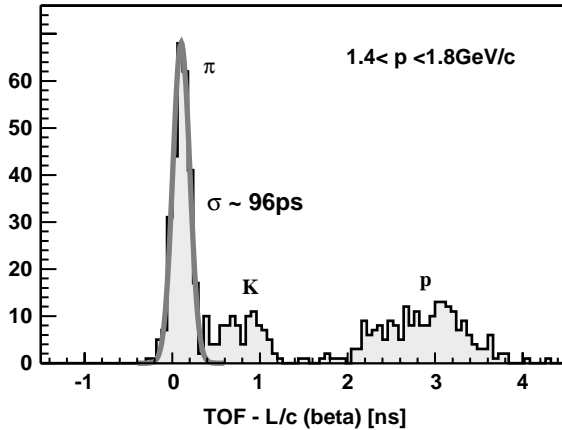


Fig. 9. The ToF resolution in the transverse momentum range $1.4 < p_T < 1.8$ GeV/c for positively charged pions. The overall ToF resolution of 96 ps is achieved.

The flight-path length of the track from the event vertex to the ToF detector as calculated by the momentum reconstruction algorithm is used to correct the ToF value measured by the ToF detector. Fig. 8 shows a contour plot of ToF as a function of the reciprocal momentum in minimum-bias Au–Au collisions after a momentum dependent track and ToF hits association residual cut between the track projection point and ToF hits has been taken. The flight path is also corrected for each particle species in this figure.

Fig. 9 shows the ToF resolution for various particles. For this example a momentum range of $1.4 < p_T < 1.8$ GeV/c for π^+ was used. The resulting ToF resolution was $\sigma = 96$ ps. Fig. 10 shows the mass-squared distribution for positive (top) and negative (bottom) charged particles integrated over all momenta. The vertical axes in these figures are in arbitrary units. The figure demonstrates that clear particle identification using the ToF was achieved in the first year of RHIC running. The timing resolution given above for the complete ToF system is achieved after slewing effect corrections and run-by-run timing offset calibrations are made.

3.5. Enhanced timing using the T0 counter

Running of the p–p experiment at PHENIX requires the use of additional systems not needed

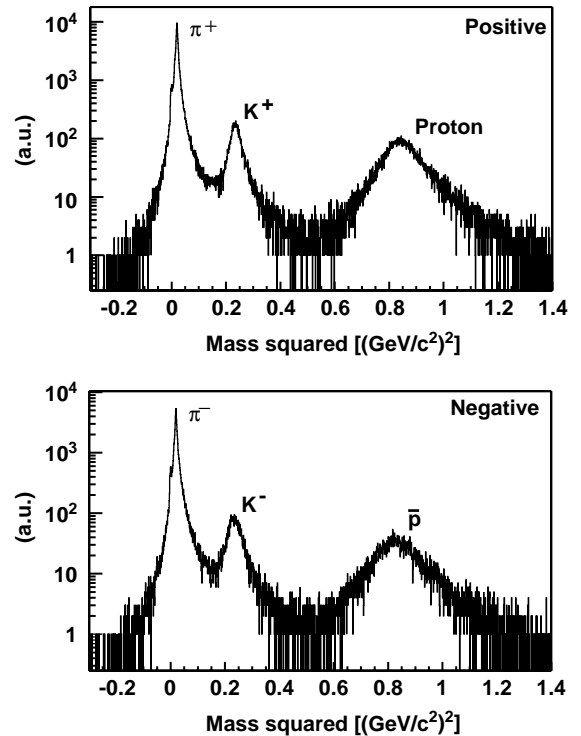


Fig. 10. Mass squared distribution for positive particles (top) and negative particles (bottom) without a momentum cutoff including all momenta. Going from left to right clear peaks for pions, kaons and protons can be seen in each panel.

for Au–Au experiments. This is necessary since the p–p collision rate is higher but on the average a collision produces far fewer hits in the BBC [8]. For this reason a T0 counter was constructed to provide precise timing for each charged particle hitting the ToF system and a Normalization Trigger Counter (NTC) described elsewhere in this volume [8] was constructed to increase the η coverage of the BBC. The T0 counter provides a precise start time for every charged particle that hits the ToF and also provides a 100% minimum bias trigger for these particles.

The T0 counter consists of a 17.5 mm thick scintillator (T0). In front of T0 is a thin Photon Conversion Rejector (PCR) consisting of a 3 mm thick scintillator. The T0+PCR is at a radius of 60 cm from the beam line and covers the full acceptance of ToF counters. T0 will provide the start time for a charged track which passes

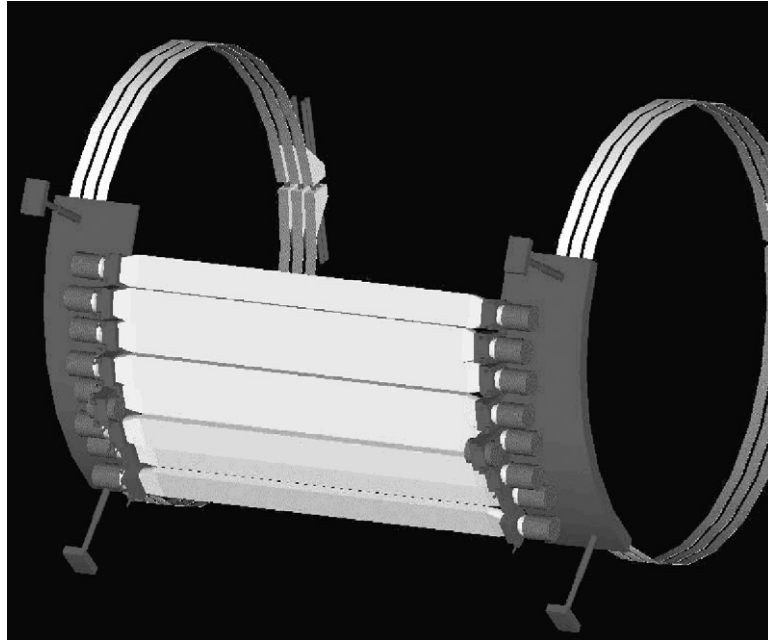


Fig. 11. Picture of the T0 counter.

through the ToF wall in order to provide particle identification for hadrons with 1–5 GeV/ c transverse momentum.

The BBC+NTC system will give a minimum bias trigger and the BBC will also give enough time-resolution for particle identification, however they will not give a 100% minimum bias trigger. To have a p–p reference for the identified charged particle distribution that can be compared with heavy ion collisions, it is essential to measure the distribution without any trigger bias. We use T0 to get the trigger and start time therefore providing the most bias-free way to measure the distribution. The T0+PCR will identify the additional photon conversion occurring in this system eliminating this additional background.

T0 consists of 8 scintillator slats (BC404) $100\text{ cm} \times 8\text{ cm} \times 17.5\text{ mm}$. Each slat has a 10 cm acrylic light guide and a Hamamatsu fine mesh PMT(H6614-01 R5924) for use in the magnetic field. The glue is optical cement (BC600). PCR consists also of 8 scintillator slats (BC404), each $100\text{ cm} \times 8\text{ cm} \times 3\text{ mm}$ thick and having 7 wave-length shift fibers (BCF92) glued in the surface of $100 \times 8\text{ cm}^2$ with BC600. 7×8 fibers on each side

are connected to the same PMT with optical grease (BC630). All the 3 mm surfaces of the PCR scintillator are painted with a reflector (BC620) and light shielding is done with aluminized mylar and black sheets. There are 80 cm of fibers outside of the PCR scintillator to provide equal light paths for the 8 counters.

Fig. 11 shows a picture of the T0/PCR detector. The T0 slats sit along the beam direction in front of the ToF acceptance and the light guide and PMT are inside the space for the inner coil. The 8 sets of T0 and PCR are placed in 7° steps and adjacent slats have 4–5 mm of overlap in ϕ to minimize dead space in the acceptance. The signals from the PMTs are fed into BBC-type FEM boards via 8 m Belden 8214 cables. The maximum HV at the PMT is -2300 V with a nominal operating HV of -2000 V or lower.

Acknowledgements

The PHENIX RICH, ToF and T0 subsystems are supported by the Japanese Ministry of Education, Science, Sports and Culture (Monbusho). We

acknowledge support from the Department of Energy (USA). RICH construction received partial support from NSF Grant 9970991 and generous machine-shop time from Florida State University.

References

- [1] K. Adcox, et al., PHENIX detector overview, Nucl. Instr. and Meth. A (2003), this issue.
- [2] K. Adcox, et al., PHENIX central arm tracking detectors, Nucl. Instr. and Meth. A (2003), this issue.
- [3] L. Aphecetche, et al., PHENIX calorimeter, Nucl. Instr. and Meth. A (2003), this issue.
- [4] W. Egle, et al., Opt. Eng. 29 (1990) 1267.
- [5] A.L. Wintenberg, et al., IEEE Trans. Nucl. Sci. NS-45 (1998) 758.
- [6] M.N. Ericson, et al., IEEE Trans. Nucl. Sci. NS-43 (1996) 1629.
- [7] S.S. Adler, et al., PHENIX on-line systems, Nucl. Instr. and Meth. A (2003), this issue.
- [8] M. Allen, et al., PHENIX inner detectors, Nucl. Instr. and Meth. A (2003), this issue.